Co-Encapsulation of Doxorubicin With Galactoxyloglucan Nanoparticles for Intracellular Tumor-Targeted Delivery in Murine Ascites and Solid Tumors

Manu M. Joseph*, S.R. Aravind*, Suraj K. George[†], Raveendran K. Pillai[‡], S. Mini[§] and T.T. Sreelekha*

*Laboratory of Biopharmaceuticals and Nanomedicine, Division of Cancer Research, Regional Cancer Centre, Trivandrum, Kerala, India; [†]Department of Hematopathology, UT MD Anderson Cancer Center, 1515 Holcombe Blvd, Houston, TX 77030, USA; [‡]Department of Pathology, Regional Cancer Centre, Trivandrum, Kerala, India; [§]Department of Biochemistry, University of Kerala, Trivandrum, Kerala, India

Abstract
Doxorubicin (Dox) treatment is limited by severe toxicity and frequent episodes of treatment failure. To minimize adverse events and improve drug delivery efficiently and specifically in cancer cells, encapsulation of Dox with naturally obtained galactoxyloglucan polysaccharide (PST001), isolated from *Tamarindus indica* was attempted. Thus formed PST-Dox nanoparticles induced apoptosis and exhibited significant cytotoxicity in murine ascites cell lines, Dalton's lymphoma ascites and Ehrlich's ascites carcinoma. The mechanism contributing to the augmented cytotoxicity of nanoconjugates at lower doses was validated by measuring the Dox intracellular uptake in human colon, leukemic and breast cancer cell lines. PST-Dox nanoparticles showed rapid internalization of Dox into cancer cells within a short period of incubation. Further, *in vivo* efficacy was tested in comparison to the parent counterparts - PST001 and Dox, in ascites and solid tumor syngraft mice models. Treatment of ascites tumors with PST-Dox nanoparticles significantly reduced the tumor volume, viable tumor cell count, and increased survival and percentage life span in the early, established and prophylactic phases of the disease. Administration of nanoparticles through intratumoral route delivered more robust antitumor response than the intraperitoneal route in solid malignancies. Thus, the results indicate that PST-Dox nanoparticles have greater potential compared to the Dox as targeted drug delivery nanocarriers for loco regional cancer chemotherapy applications.

Translational Oncology (2014) **7**, 525–536

Introduction

Drug-induced toxicity is a serious problem affecting patients undergoing chemotherapy. Depending on the toxicity profiles of individual drugs, therapeutic index may be limited, resulting in higher rate of treatment failures [1]. Apart from toxicity, cancer cells also acquire self-remedial escape mechanisms such as drug efflux pumps or increased drug metabolisms devouring attack from chemotherapy, resulting in the chemoresistance [2].

Doxorubicin (Dox) is a common chemotherapeutic drug with wide spectrum of anticancer activity against several malignancies. But, the most common side-effects associated with anthracycline analogues like Dox include acute and chronic toxicities such as myelosuppression, cardiomyopathies and congestive cardiac failure [3,4]. To overcome these side-effects, integrated approaches utilizing combination therapies with cytotoxic, chemosensitizing and nanoparticle agents have been devised. Encapsulation of Dox in the form of PEGylated liposomes (Doxil) and Abraxane have increased the

intratumoral delivery without much toxicity [3,5]. Dox conjugation with hydrophilic polymers was found to increase cytotoxicity by 'enhanced permeation and retention' (EPR) relative to free doxorubicin [6]. EPR effect enabled polymeric-drug nanoparticles to enhance their diffusion rate, and thus accumulate within tumor tissues than normal tissues, leading to enhanced antitumor efficacy and reduced side-effects. A small number of advanced drug delivery systems for Dox have been approved by the FDA for the treatment of ovarian cancer and Kaposi's sarcoma which are in clinical use in the United States [7]. Still, there are substantial challenges like high treatment failure rates, unpredictable disease outcome, and tumor recurrence apart from toxicity, while using any single-agent drugs.

In this scenario, naturally obtained polymeric nanoparticles are important where they are utilized for the diagnosis and treatment of a wide range of diseases including cancer. In the purlieu of cancer therapeutics, polymeric nanoparticles are considered as novice drug systems. But, in fact they are credible tumor targeting agents because of their ability to sustain the conjugated drugs in circulation and retain enhanced drug uptake *via* enhanced permeation and retention effect [8–10]. They could be easily surface engineered to function precisely over different types of architecture, shape, size, surface charges across all the barriers for the optimal drug delivery [11,12]. However, strategies to co-encapsulate multiple drugs during the synthesis of nanoparticles are always challenging. Physical loading, chemical conjugation and covalent linkage of the drugs to the polymer backbone has often been the method of choices [13–16]. But, several other factors such as steric hindrance, heterogeneity and variable drug reactions interfere, and pose a major challenge during synthesis [17]. Majority of the polymeric nanoparticles are polymeric micelles which are electrically neutral, capable of evading drug clearance by the reticulo-endothelial systems, and are frequently used against murine solid tumors [18]. In combination with Dox, they appear effective and safe [19]. Apart from being biocompatible, polymeric nanocarriers also demonstrate favorable pharmacokinetics [20].

We previously isolated and characterized naturally obtained PST001 (Galactoxyloglucan) from the seed kernels of *Tamarindus indica* (Ti) [21]. PST001 has been demonstrated to show excellent antitumor and immunomodulatory activity against various cancers *in vitro* and *in vivo* [21–23]. Another nanoparticle formulation of PST001 and gold (PST-Gold) developed in our laboratory demonstrated superior cytotoxic and immunomodulatory activity compared to the parent polysaccharide [24,25]. PST001 in conjugation with Dox also elicited significant anticancer activity in breast, leukemic and colon cancer cells *in vitro* [26]. However, in order to determine the versatile nature of this nanoconjugate anticancer drug in aggressive cancers like lymphoma, current study was aimed to evaluate the potential of PST-Dox in murine ascites and solid tumors. In addition, the most effective drug delivery routes of this nanoparticle derivative and the rate of Dox internalization from the nanoparticle conjugates in the human breast, leukemic and colon tumor sites were also determined. For this purpose, we synthesized and chemically characterized nanoparticle conjugated PST001 and Dox (PST-Dox), and tested its anti-tumor activity *in vitro* and *in vivo*. Our results suggest that the PST-Dox exhibited excellent cytotoxicity, apoptotic and antitumor activities in either forms of ascites tumors. Specifically, nanoconjugates decreased tumor volume, viable tumor cell counts, and increased overall survival in mice during the early as well as established stages of the disease. Further, our studies also demonstrate that intratumoral nanoparticle drug delivery is an effective choice over intraperitoneal route in combating aggressive solid malignancies.

Materials and Methods

Modification of Doxorubicin and Characterization of PST-Dox Nanoparticles
Ripened seeds of Ti were obtained from reliable sources. The seeds were dried and powdered, and the polysaccharide, PST001 was isolated as previously reported [21,23,24]. The carbohydrate content was determined by Duboi's method [27] using D-glucose as the standard. The PST-Dox nanoparticles were prepared by ionic gelation of PST001 and Dox using sodium tripolyphosphate (TPP) and the final product was lyophilized and stored at 4°C until use. All procedures were performed with minimal exposure to light.

Cell Lines
The murine lymphoid cancer cell lines Dalton's lymphoma ascites (DLA) and Ehrlich ascites carcinoma (EAC) were procured from Amala Cancer Research Centre, Thrissur, India. Both DLA and EAC cell lines were maintained in the peritoneal cavity of mice by intraperitoneal serial transplantation of 1×10^6 cells/mice. The human cancer cell lines MCF-7 (breast cancer) and K562 (leukemia) were obtained from the National Centre for Cell Sciences, Pune, India. The colon cancer cell line HCT116 was generously provided by the RGCB (Rajiv Gandhi Centre for Biotechnology), Thiruvananthapuram, India. The cells were maintained in DMEM media with 10% fetal bovine serum and 5% CO_2 at 37°C.

In Vitro Cytotoxicity Assay
The growth inhibitory capacity of the PST-Dox nanoparticles on murine cancer cell lines, DLA and EAC cells were evaluated by MTT (3-[4, 5-dimethylthiazol-2yl]-2, 5 diphenyltetrazolium) assay [28]. The absorbance was measured at 570 nm using a microplate spectrophotometer (BioTek, Power Wave XS). MTT assays were performed on cancer cell lines upon treatment with PST001, PST-Dox nanoparticles and Dox with varying concentrations ranging from 0.0001 ng/ml to 100 µg/ml over a period of 24 to 48 hours.

Acridine Orange-Ethidium Bromide Double Staining Assay
Acridine orange-ethidium bromide double staining assay is a rapid and inexpensive assay to detect apoptotic damages, based on the differential uptake of two fluorescent DNA binding dyes by viable and nonviable cells [29]. Briefly, control or PST-Dox treated DLA and EAC cells were treated for 24 hours and double-stained with acridine orange and ethidium bromide. The changes in fluorescence in these cells were observed under an inverted fluorescent microscope using a FITC filter (Olympus 1X51, Singapore).

Quantification of Cellular Uptake and Retention of Dox
Estimation of cellular uptake of Dox in human cancer cell lines, HCT116, MCF7 and K562 was performed as described elsewhere [30,31] with slight modifications. Briefly, cells were plated onto 12-well plates at 10^5 cells/well and incubated in a 5% CO_2 incubator at 37°C. When the cells attained confluence, they were treated with vehicle or PST-Dox or Dox, and incubated for 4 h, trypsinized and washed with ice-cold phosphate buffered saline (PBS, pH 7.4). Pellets were lysed again with PBS containing 1% Triton-X accompanied with rigorous vortexing. The supernatant collected were centrifuged at

10,000 rpm for 4 min and the concentration of Dox in the cell lysates was measured in a fluorometer (FLx800, BioTek) at an excitation wavelength of 485 nm and an emission wavelength of 590 nm. Results are expressed as micrograms of Dox per milligrams of cellular protein. Protein concentration of the cell lysates was determined using Coomassie plus protein assay reagent and bovine serum albumin as standards (Pierce, Rockford, IL, USA).

Visualization of Cellular Dox Uptake by Confocal Microscopy

Confocal fluorescence microscopy was used to observe the intracellular uptake and distribution of Dox from PST-Dox nanoparticles and the standard Dox. Adherent cancer cells (HCT116 and MCF-7) were grown overnight in 12 mm circular glass coverslips with 10 % DMEM for 24 hours. Cells were incubated with PST-Dox nanoparticles (1 μg/ml) for 2 h and 6 h or Dox (1 μg/ml) for 6 h. The cells in the cover slips were fixed with 4% paraformaldehyde, counterstained with DAPI and mounted with DPX on a clean glass slide. Slides were observed under a fluorescence confocal microscope (NIKON A1R, USA) and were analyzed using NIS Elements software. The confocal microscopy settings were kept the same between samples. Doxorubicin excitation and emission occurred at 485 nm and 595 nm whereas for DAPI, excitation and emission occurred at 405 nm and 450 nm respectively. Images were acquired in 60x optical zoom (Plan Apo VC 60x Oil DIC N2 DIC N2).

Experimental Design for Ascites Tumors In Vivo

Female BALB/c mice were maintained in well-ventilated cages with free access to normal mouse food and water provided *ad libitum*. Temperature (25 ± 2℃) and humidity (50 ± 5%) was regulated and the illumination cycle was set to 12 h light/dark. Animal protocols were reviewed and approved by Institutional Animal Ethics Committee (IAEC) and Committee for the Purpose of Control and Supervision of Experiments on Animals (CPCSEA), India and the experiments were performed as summarized in Figure 1. Briefly, animals were divided into four groups. All groups had mice inoculated with either DLA or EAC on Day 1, except for group 4, where the cells were injected on Day 8.
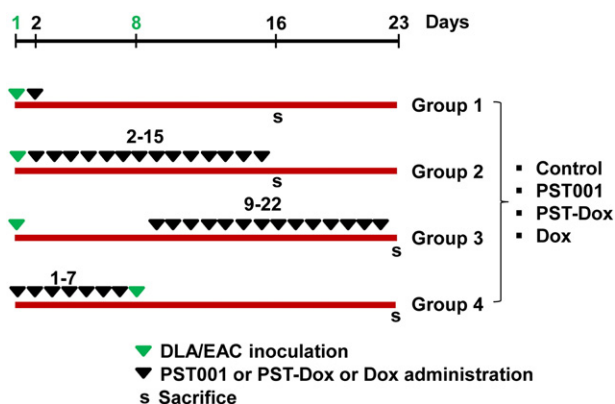

Figure 1. Schematic for *in vivo* DLA and EAC ascites tumor models. Female mice were intraperitoneally transplanted with DLA or EAC ascites tumors on day 1 or day 8 and divided into four groups as shown, depending on the treatment schedule. Each of these groups has been subdivided into four subgroups (n = 6/subgroup) – Control (PBS), PST001, Dox and PST-Dox. Compounds were administered on different days as shown. Mice were sacrificed to estimate antitumor parameters on day 16 (group 1 and 2) or day 23 (group 3 and 4).

Group 1 was treated only once (day 2) with compounds. In group 2, compounds were administered on days 2 to 15. Group 3 had compounds administered on days 9 to 22. Group 4 received prophylactic treatment of compounds from day 1 to 7. Each of these groups had four treatment protocols – PBS (vehicle or control), PST001 (100 mg/kg), PST-Dox nanoparticles (2.25 mg/kg) and Dox (2.25 mg/kg) under subgroups (n = 12/sub group). Six animals from the group were used for survival analysis. Vehicle and the compounds were administered once daily by *intraperitoneal* (*i.p.*) injection. The mean survival time and percentage of increment in life span (% ILS) was calculated as previously reported [25,32].

EAC-Induced Solid-Tumor Mice Syngraft In Vivo

EAC cells ($1{\times}10^6$ cells) were injected subcutaneously with a fine needle (31G) to develop solid tumors in the hind limb of mice (n = 6/group). These experiments utilized administration of compounds - PST001, PST-Dox nanoparticles and Dox by two different routes, *intraperitoneal* (*i.p.*) and *intratumoral* (*i.t.*) injections, daily for 14 consecutive days, starting on day 9 after tumor inoculation (days 9 to 22 as shown in Figure 1, Group 3). Animals were sacrificed on day 23 to determine tumor volume and overall survival (n = 6/subgroup). The radii of the developing tumors were measured every third day from day 7 to day 31, using vernier calipers and the tumor volume was estimated using the formula: $V = 4/3\pi r_1^2 r_2$, where r_1 and r_2 represent the radii from two different sites [25,32,33].

Statistical Analysis

Data are expressed as the mean ± standard deviation (SD) of three replicates and analyzed using GraphPad PRISM software 5.0 (GraphPad Software Inc., San Diego, CA). One-way analysis of variance was used for the repeated measurements, and the differences were considered to be statistically significant if $P < .05$. SPSS 17.0 statistical software (IBM Inc., NY) was used for Kaplan-Meier survival analysis. The IC_{50} values were calculated using the Easy Plot software (Spiral Software, MD).

Results and Discussion

Synthesis and Cytotoxic Effects of PST-Dox Nanoparticles

The polysaccharide PST001 isolated from the seed kernels of Ti was found to have neutral pH with total sugar content of 98%, as determined by the phenol-sulfuric acid method. After isolation, the polysaccharide was purified by gel filtration chromatography, lyophilized and stored at 4℃. Ionic gelation was utilized to produce the PST-Dox nanoparticles with an average size of 10 nm; nanoconjugates were lyophilized and stored with minimal exposure to light [26]. PST-Dox nanoparticles were evaluated for cytotoxic activity against two murine ascites cancer cell lines, DLA and EAC by MTT assay. The cytotoxic potential was found to be highly significant in both the cell lines examined (Figure 2A and B). DLA and EAC cells were growth-arrested with IC_{50} values of 0.58 ± 0.4 μg/ml and 0.42 ± 0.3 μg/ml, respectively after 24 hours of incubation with PST-Dox nanoparticles. Dox alone generated IC_{50} values of 6.37 ± 1.2 μg/ml (DLA) at 48 h, and 80 ± 1.4 μg/ml (EAC) at 24 hours. The native polysaccharide PST001 produced IC_{50} values of 43 ± 1.3 μg/ml (DLA) and 597 ± μg/ml (EAC) only after prolonged hours (48 h) of incubation (Figure 2, A and B). Earlier, we showed the potency of PST-Dox against other cancer cell lines such as MCF-7, HCT116 and K562 cells [26].
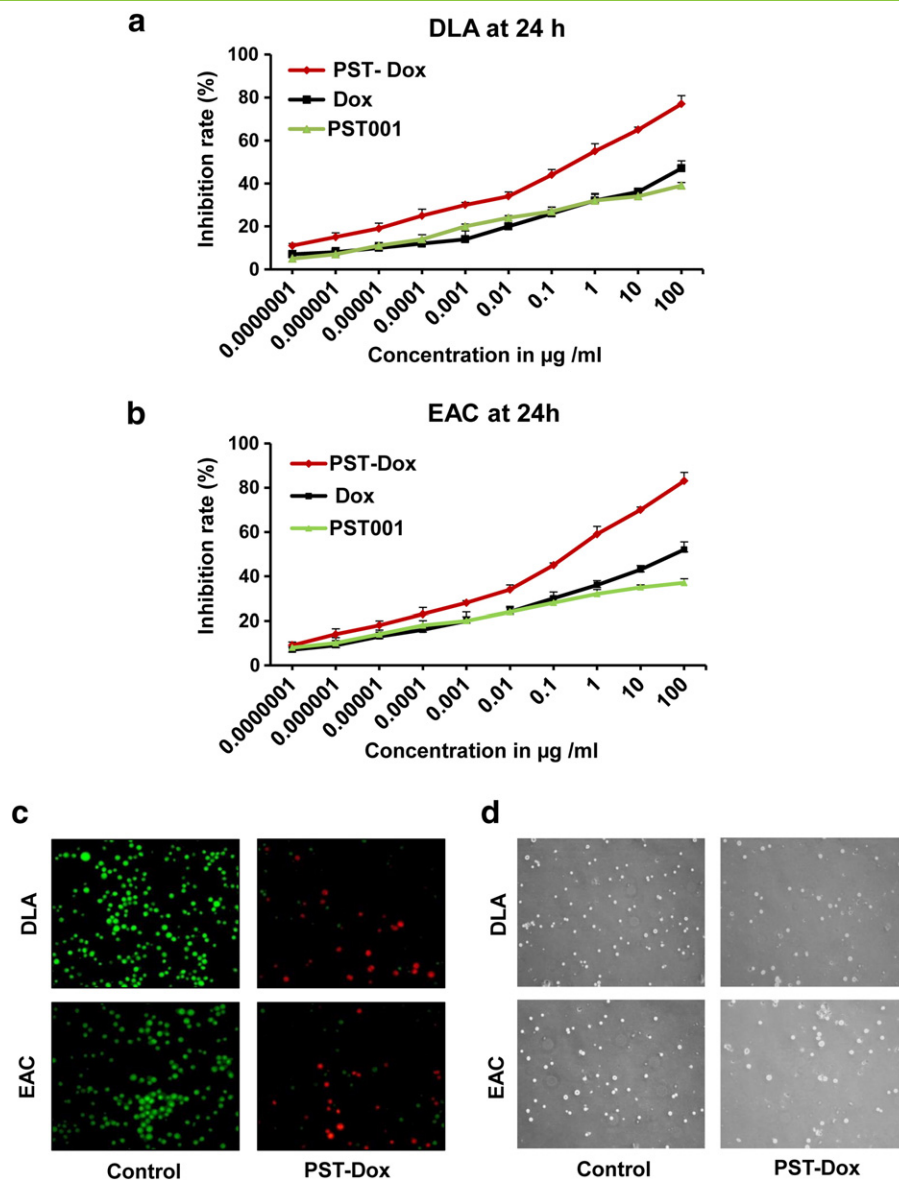
Figure 2. Evaluation of cytotoxicity and apoptosis in PST-Dox nanoparticles treated DLA and EAC cells.Inhibition of cell proliferation rates were determined by MTT assay at 24 hours for (**a**) DLA and (**b**) EAC cells. Results were expressed as the mean ± SD from three independent experiments. Representative fluorescent images of apoptosis evaluation of cell lines treated with vehicle (PBS) or 1 μg/ml PST-Dox nanoparticles for 24 hours by **(c)** Acridine Orange- Ethidium Bromide dual staining in DLA and EAC cells. Phase contrast microscopy images are shown in **(d)** DLA and EAC cells treated with vehicle or PST-Dox nanoparticles.

With more concrete evidence, it is now imperative to say that the new Dox formulation with PST001, PST-Dox also exhibits wide spectrum of anticancer activity with even better effects than PST001 or Dox as single agents alone. This could be partly due to the cytotoxic effects elicited by the already known cytotoxic agents, PST001 and Dox. In addition to the synergistic effect, the increased surface-to-volume ratio of the nanoparticles permitted PST-Dox with optimal physical, chemical, and biological activities compared with its parent macromolecules. Further, the synthesis of PST-Dox involves the polyanion, TPP as the linker. PST001 being neutrally charged and consisting of numerous hydroxyl groups provide anchors for drug attachment and modification. This enables easy binding with TPP, and further with the positively charged Dox-HCl. This nanoconjugate was previously tested to provide a Dox-encapsulation efficiency of 70% as reported [26]. The release profile of Dox from

the PST-Dox nanoparticles and Dox-HCl at different pH levels over time at ambient temperature was also previously evaluated [26]. It was found that doxorubicin hydrochloride showed a burst release within 3–5 hours regardless of the change in pH from 4.5 to 7.4. However, the PST-Dox nanoparticle showed excellent pH and time dependent Dox release kinetics. Yet, another nanoformulation of PST001 with gold (PST-Gold) also demonstrated similar kinetic profiles and exhibited superior anticancer potential [24].

PST-Dox Nanoparticles Exert Anticancer Effects Through the Induction of Apoptosis

To determine the mechanism of cell death induced by the PST-Dox nanoparticles in cancer cells, apoptotic assays were conducted after the administration of 1 μg/ml of nanoparticles for 24 hours. Compared to the controls, acridine orange-ethidium bromide

staining in the cells treated with the PST-Dox nanoparticles showed a drastic change in fluorescence from green to yellow/red that was associated with other apoptotic features such as the presence of apoptotic bodies and nuclear condensation. Significant changes in fluorescence were observed in both DLA and EAC cells upon treatment with PST-Dox nanoparticles (Figure 2C). Morphological and phase contrast microscopy evaluation of cells treated with PST-Dox nanoparticles (1 μg/ml) for 24 hours showed salient features of apoptosis such as distorted shape, membrane blebbing, and the presence of apoptotic bodies compared to the vehicle in DLA and EAC cells (Figure 2D).

Apoptosis is the most appropriate mode of cell death in living systems induced by several polysaccharides [34], anticancer drugs such as doxorubicin [35] and polysaccharide based nanoparticles [24]. Membrane blebbing, one of the hallmarks of apoptosis refers to the irregular bulges in the plasma membrane of the cells caused by localized decoupling of the cytoskeleton from the plasma membrane. PST-Dox also exhibited similar trends of apoptosis in MCF-7, K562 and HCT116 as reported earlier [26]. In the current study, the inhibition of cell proliferation exhibited by the PST-Dox nanoparticles in the lymphoma was confirmed through the induction of apoptosis. The extended efficiency of the PST-Dox nanoparticle compared to PST001 and Dox in inducing apoptosis may have been due to the increased uptake of the particles *via* endocytosis because of small size and increased surface-to-volume ratio [36].

Dox is Internalized Efficiently From PST-Dox Nanoparticles in Human Cancer Cells

Although DLA and EAC models exhibited robust anticancer effects, cellular uptake and retention assays were not possible in ascites tumors as per the standardized protocols. However, it was relevant to evaluate the internalization of Dox from the nanoconjugates in clinically applicable human cancer cells. Hence, an established protocol mimicking clinical scenario in human cancer cell lines such as HCT116, MCF-7 and K562 was utilized for the measurement of intracellular Dox. Intracellular incorporation of Dox measured in HCT116 (Figure 3A) and MCF-7 (Figure 3B) by confocal fluorescence microscopy revealed a significant and visible increase in the doxorubicin uptake in the nanoparticle treated cells compared with naked Dox. There occurred a time dependent increase in the doxorubicin fluorescence with PST-Dox nanoparticles, where 6 hours of administration showed more visible internalization than at 2 hours in all the three cell lines examined. However, 2 h of incubation with PST-Dox nanoparticles showed more fluorescence than naked Dox for 6 h in both HCT116 and MCF-7 cells. Vehicle-treated cells showed well integrated nucleus with the DAPI staining in all the cells. Distortion of the nuclear material was observed on administration of both Dox and PST-Dox nanoparticles, indicating the cytotoxic effect on cancer cells. Quantification of the cellular Dox uptake by fluorimetric estimation of HCT116 and MCF-7 cell lines treated with 1 μg/ml of either Dox or PST-Dox nanoparticles for 4 hours revealed a significant increase in
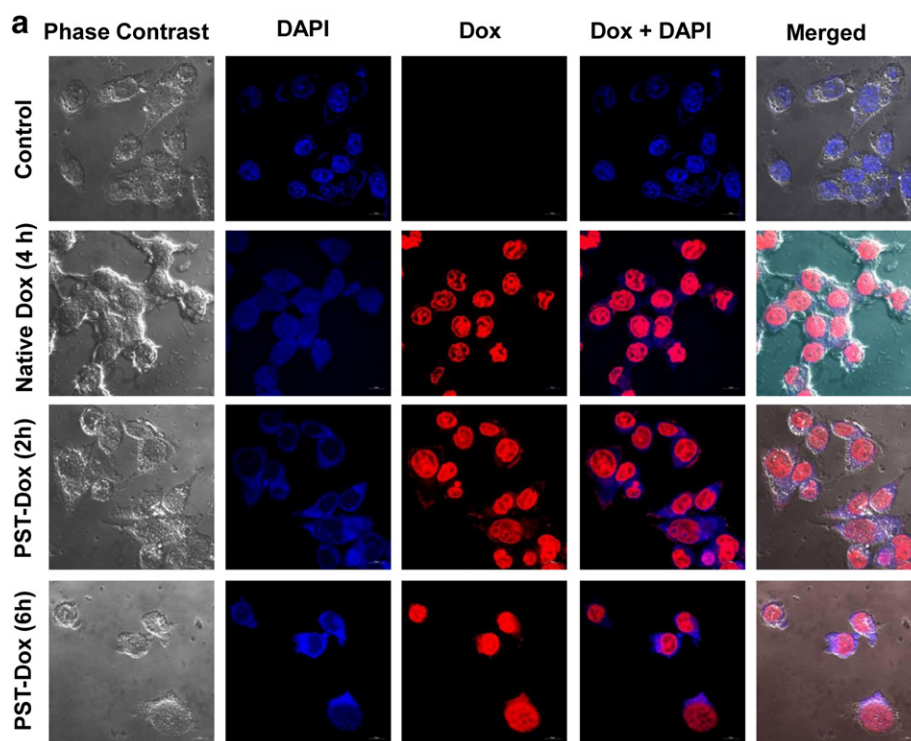

Figure 3. Intracellular doxorubicin uptake by human cancer cells.Confocal fluorescence microscopy was used to evaluate the intracellular uptake and distribution of Dox in **(a)** HCT116 and **(b)** MCF-7 cells. Representative images of these cells treated with vehicle (control), standard clinically used Dox (1μg/ml at 4 h) or PST-Dox nanoparticles (1 μg/ml) at 2 h (second to last row) or 6 h (last row). First column represents the phase contrast microscopy images and the consecutive columns represent DAPI, Dox, DAPI+Dox overlay and merged images **(c)** Quantitation of Dox uptake in HCT116, MCF-7 and K562 cells was determined fluorimetrically at an excitation wavelength of 485 nm and an emission wavelength of 590 nm in the presence of either Dox (1 μg/ml) or PST-Dox nanoparticles (1 μg/ml). Statistically significant differences at a, p<0.001 compared to corresponding control group.
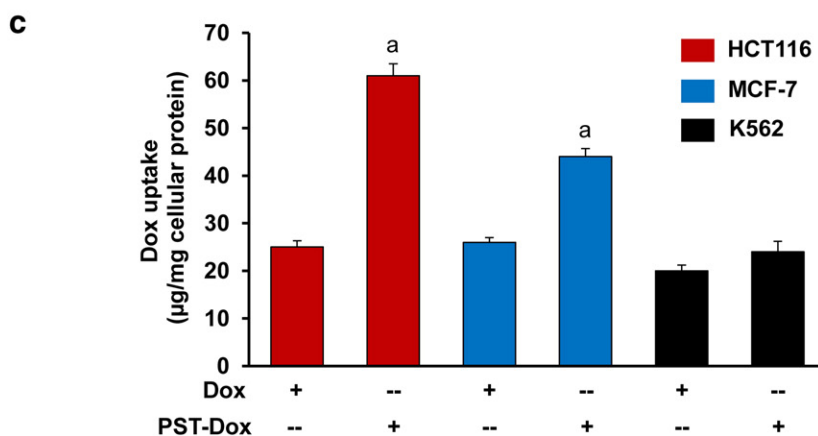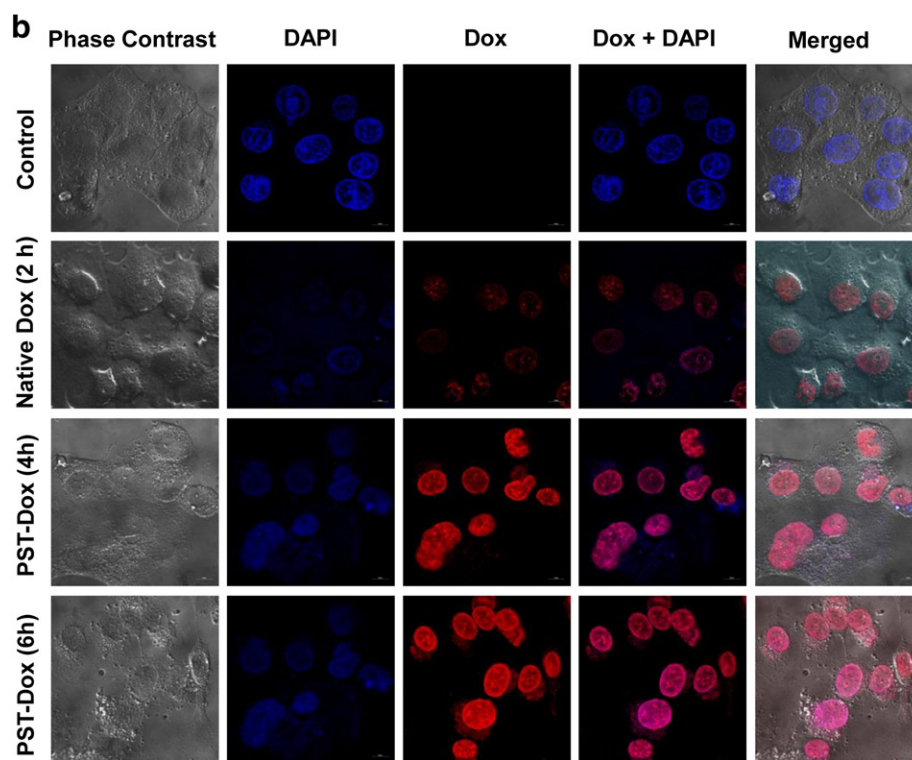
Figure 3. *Continued.*

Dox uptake from the nanoparticles when compared with the free drug, Dox (Figure 3*C*). HCT116 cells showed the maximum Dox uptake of 61 ± 2.5 μg/mg cellular protein from the nanoparticles, while the native Dox showed only 25 ± 1.3 μg/mg cellular protein. MCF-7 and K562 cells exhibited uptake of 44 ± 1.7 μg and 24 ± 2.2 μg of doxorubicin/mg cellular protein respectively from the nanoparticles. However, relatively lesser quantity of doxorubicin was internalized from the naked Dox; 26 ± 1 μg (MCF-7) and 20 ± 1.2 μg (K562) per mg of cellular protein (Figure 3*C*).

The increased cytotoxicity observed with PST-Dox nanoparticles than the native drug even at lower concentrations and lesser incubation periods was evident through the increased uptake of the nanoparticles by the cancer cells. PST-Dox nanoparticles showed a rapid uptake into the cancer cells within a short period of incubation. Conventionally, nanoconjugates of polymers release drugs in a favorable manner either *via* diffusion of the drug moieties through the polymer matrix or *via* differential surface erosion rates of the nanoparticles. The enhanced uptake of the PST-Dox nanoparticles than the parental Dox by the cancer cells could be due to the EPR effect exhibited by the nanoparticles by virtue of their increased surface-to-volume ratio and small size [37].

Increased uptake visibly observed with the confocal microscopy was consistent with the quantitation of fluorimetric estimation in all the cancer cells. The favorable properties exhibited by PST-Dox nanoparticles in terms of increased cancer specific cytotoxicity and minimal toxicity towards normal cells could be attributed to the higher intracellular accumulation and deeper penetration of the nanoparticles into the cancer cells. Delivery of the anthracycline doxorubicin in tumor cells was indeed sub-optimal in its unmodified form due to its non-specific distribution in the untargeted regions,
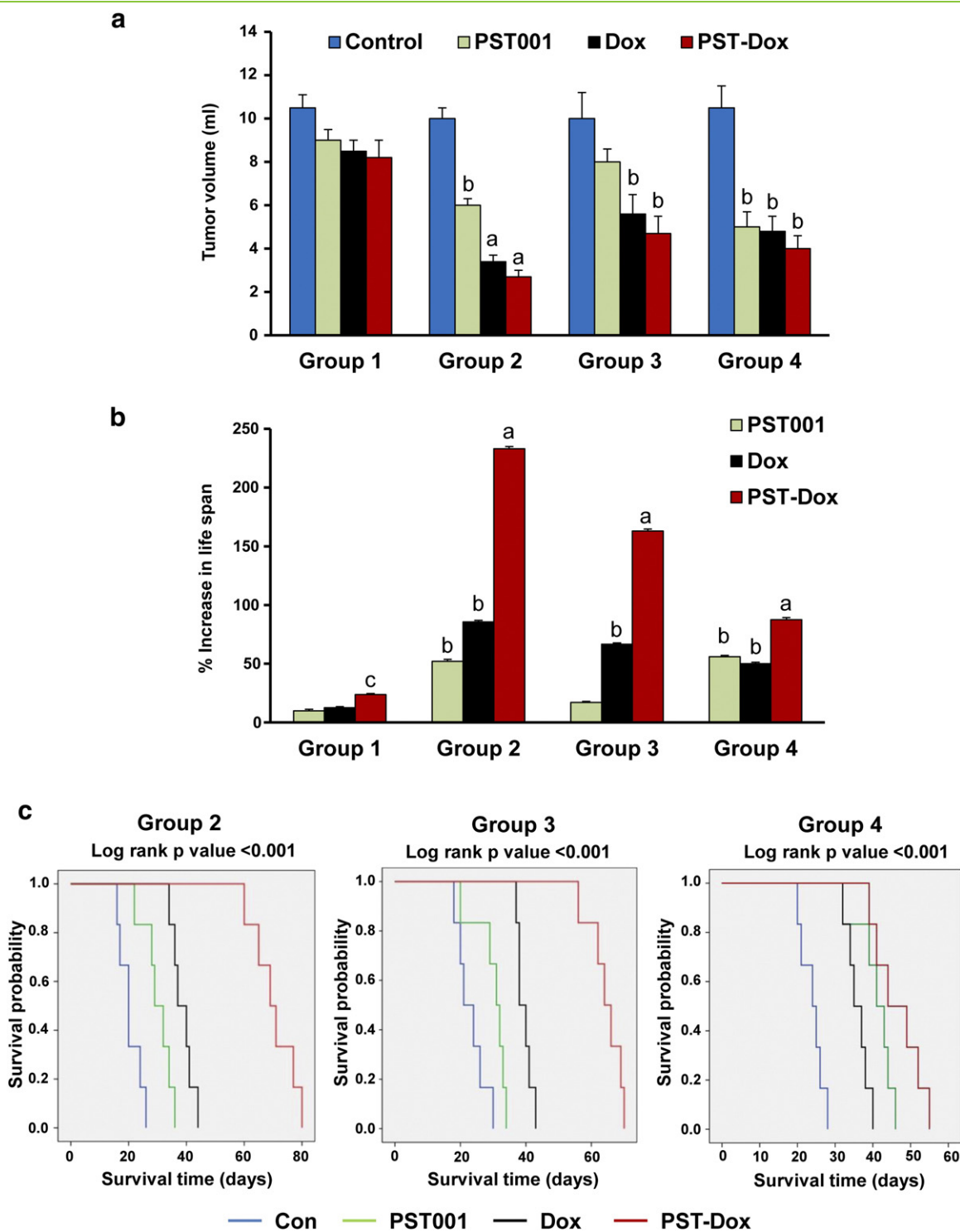
Figure 4. Antitumor effects of parent compounds and nanoparticles in DLA mice.**(a)** Ascites tumor volume measurements were taken from the different treatment groups/subgroups at the end of experimental period **(b)** Percentage increment in the life span in DLA mice treated with various compounds. Results are expressed as the mean ± SD of the group. Statistically significant differences at a, $P < .0001$; b, $P < .001$ and c, $P < 0.01$ compared to corresponding control group. **(c)** Kaplan-Meier survival curves of DLA-tumor mice treated with different compounds in group 2, group 3, and group 4. Significance shown is for PST-Dox mice *vs.* corresponding control group.

and hence severe side effects were observed [38]. Our *in vivo* studies have previously reported the tumor-specific bioaccumulation of the nanoparticles [26] and the current *in vitro* data presented here establish that PST-Dox nanoparticles readily delivers Dox into the human cancer cells as early as 2 h after administration, probably owing to its small size compared with the clinically used analogue.

PST-Dox Nanoparticles are Effective Against Early, Established and Highly Recurrent Stages of Ascites Tumors

In spite of the robust efficacy exhibited by the PST-Dox *in vitro*, we next evaluated antitumor effects *in vivo* in order to establish the therapeutic utility. DLA and EAC ascites tumor-bearing mice were evaluated on the 16th and 23rd day of the compound administration

Table 1. Assessment of antitumor parameters in group 2.

Parameter	DLA				EAC			
	Control	PST001	Dox	PST- Dox	Control	PST001	Dox	PST- Dox
Tumor volume (ml)	10 ± 0.5	6 ± 0.3[a]	3.4 ± 0.3[a]	2.7 ± 0.3[a]	11 ± 1.0	5.5 ± 1.0[a]	3.4 ± 0.5[a]	3 ± 0.4[a]
Body weights (g)	33 ± 1.2	29 ± 1.1	22 ± 0.9[a]	29 ± 0.6	34 ± 0.7	30 ± 1.0	23 ± 1.3[a]	29 ± 0.8
TCC (10^6 cells/ml)	166 ± 2.1	88 ± 1.9[a]	56 ± 1.0[a]	44 ± 0.8[a]	175 ± 1.2	82 ± 0.8[a]	54 ± 0.7[a]	47 ± 1.0[a]
% VTCC (10^6 cells/ml)	95 ± 1.9	75 ± 0.9[a]	49 ± 0.6[a]	42 ± 1.0[a]	94 ± 1.0	72 ± 1.0[a]	45 ± 1.5[a]	43 ± 1.3[a]
MST (days)	21 ± 1.1	29 ± 1.9[a]	39 ± 1.4[a]	70 ± 1.0[a]	20 ± 1.0	27 ± 1.4[a]	35 ± 1.2[a]	68 ± 0.9[a]
% ILS	0.0	52 ± 1.7[a]	85.7 ± 1.2[a]	233 ± 1.9[a]	0.0	50 ± 1.0[a]	75 ± 1.4[a]	240 ± 1.8[a]

Evaluation of various parameters in mice injected with DLA or EAC cells on day 1 followed by compound administration on days 2 through 15 (group 2). Data are expressed as mean ± SD (n = 6). Statistically significant differences at a, $P < .001$ compared to respective control group. TCC – Tumor cell count; VTCC – Viable tumor cell count; MST – Mean survival time, ILS – Increment in life span.

for the effects on body weight, tumor volume, viable and non-viable tumor cell counts, and % ILS. Body weights were proportional to the age in weeks demonstrating no significant differences except in mice treated with Dox (Table 1 for group 2; for others data not shown). Tumor reduction in DLA-bearing mice in terms of tumor volume was evident in all the groups except group 1 in comparison to the control group (Figure 4A; Table 1; Supplementary Tables 1 and 2). Tumor reduction was highly significant in PST-Dox treated mice in group 2 ($P < .0001$), followed by group 4 ($P < .001$) and group 3 ($P < .001$) in comparison to the control. Dox treatment also reduced DLA tumor volume significantly in at least three groups (group 2, $P < .0001$; group 4, $P < .001$; group 3, $P < .001$ vs. control). Although PST001 as a single agent was effective, reduction in tumor volume was significant only in group 4 ($P < .001$) and group 2 ($P < .001$). As noted above, the compounds failed to reduce the tumor volume significantly in group 1, probably owing to a single day treatment regimen after tumor inoculation. Likewise, as observed in tumor reduction, % ILS was also highly significant in PST-Dox treated group 2, followed by group 3 and group 4 (all three groups at $P < .0001$ vs. control) (Figure 4B; Table 1; Supplementary Tables 1 and 2). Dox was also effective in increasing the life span in group 2, group 3 and group 4 (all three groups at $P < .001$), while PST001 was significant in group 4 and group 2 ($P < .001$). However, it is significant to note that PST-Dox also increased the life span in group 1 mice bearing DLA tumor ($P < .01$). The Kaplan-Meier survival curves of DLA mice treated with PST001, Dox or PST-Dox nanoparticles in different groups are shown in Figure 4C. PST-Dox treated mice group was highly significant ($P < .001$ vs. control), followed by Dox ($P < .01$) and PST001 ($P < .01$). Just as in the group 4, PST001 was slightly better than Dox with respect to the survival curves.

A similar trend showing tumor reduction was also seen in the EAC-bearing mice in all groups except group 1 (Figure 5A; Table 1; Supplementary Tables 1and 2). PST-Dox had the best effect compared to other compounds in reducing EAC tumor in the majority of the treatment regimen. Group 2 showed the highest effect ($P < .0001$) in terms of tumor volume reduction, followed by group 3 ($P < .001$) and group 4 ($P < .001$) compared to the respective control mice. Treatment with Dox was also effective in group 2 ($P < .0001$), followed by group 4 ($P < .001$) and group 3 ($P < .001$). PST001 alone was the least effective ($P < .001$ vs. respective control) among the three treatment groups which showed some tumor reduction. In EAC-bearing tumor mice, a maximum ILS of 240 ± 1.8% was observed on PST-Dox nanoparticle administration in group 2 (Figure 5B; Table 1; Supplementary Tables 1 and 2). Increment in the lifespan was highly significant in PST-Dox treated groups 2 and 3 ($P < .0001$ vs. control) followed by group 4 ($P < .001$ vs. control). ILS percent also corresponded with tumor reduction in nanoparticle treated mice. Although not comparable with PST-Dox, Dox also prolonged life span in groups 2, 3 and 4

($P < .001$ vs. control). As seen earlier, PST001 was the least effective drug with ILS around 54% in group 4, followed by group 2 (both groups at $P < .001$ vs. control). Group 1 treatment regimen did not have significant improvement with respect to ILS in all the three drugs tested which is consistent with the tumor reduction seen in EAC cells. The Kaplan-Meier survival curves of EAC groups are shown in Figure 5C. PST-Dox treatment was highly significant in groups 2, 3 and 4 compared to the corresponding control group ($P < .001$). Like in the previous data sets, Dox treatment ($P < .01$) was the next significant group, followed by PST001 in the Kaplan-Meier survival curves.

In the ascites tumor models, it is clear that PST-Dox showed the best overall effect, especially when administered for several days before and after tumor inoculation. This points to the fact that PST-Dox is indeed efficient against tumors those are recently transplanted (days 2–15), established (days 9–22) or have chances of recurrence (days 1–7). In the clinical scenario, this is relevant because the drug could be effective in early, established and resected stages of the disease. Another aspect of this nanoconjugate is that they are a safer alternative compared to the parental Dox. In our studies, PST-Dox nanoparticles was found to be safer in animals with no indication of side-effects during the entire course of experiments in both the DLA and EAC ascites tumor models (Supplementary Figure 1). Even though Dox administration was effective and reduced the tumor burden, it was predominantly laden with visible signs of toxicity (Supplementary Figure 1). Majority of the animals treated with Dox showed severe weight loss, alopecia and cachexia, whereas PST-Dox treated mice appeared normal with no apparent signs of toxicity.

Intratumorally Administered PST-Dox Nanoparticles are More Efficient Against Solid Malignancies

We next evaluated the antitumor activity of PST-Dox nanoparticles in a syngenic EAC-induced solid-tumor mice syngraft. There was a significant reduction in the tumor burden observed as early as day 13 (intratumoral) or day 16 (intraperitoneal), on different routes of PST-Dox administration. Both i.p. (Figure 6A, Supplementary Table 3) and i.t. (Figure 6B, Supplementary Table 3) routes showed significant solid tumor reduction starting from days 13 or day 16 ($P < .001$ vs. respective control) on treatment with PST-Dox nanoparticles. For the intratumoral drug treatment, statistical significance ($P < .001$ vs. control) was achieved from day 19 (Dox) and day 25 (PST001) for the parent compounds. For intra-peritoneal drug treatment, solid tumor reduction was statistically significant ($P < .001$ vs. control) from day 19 (Dox) and day 25 (PST001). As expected in the control group, the size of solid tumor increased as the days progressed and the tumor burden was 3.7–5.6-fold higher compared to the PST-Dox treated mice at the end of 31
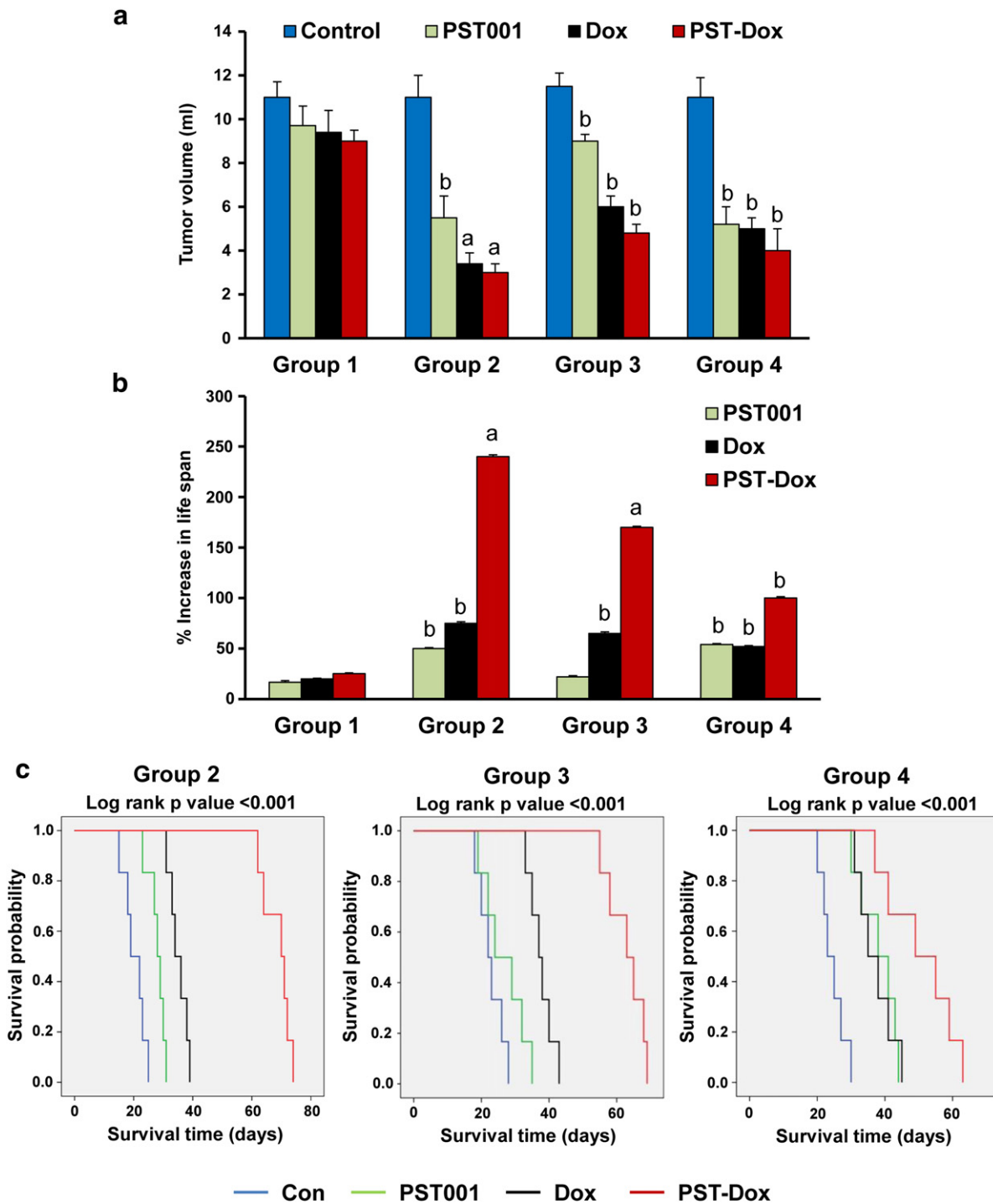
Figure 5. Antitumor effects of parent compounds and nanoconjugates in EAC mice. **(a)** EAC ascites tumor volume was measured in different treatment groups/subgroups at the end of experimental period **(b)** Percentage increment in the life span in EAC mice treated with various compounds. Data are expressed as mean ± SD of all mice in the group. Statistically significant differences at a, $P < .0001$ and b, $P < .001$ compared to corresponding control group. **(c)** Kaplan-Meier survival curves of EAC-tumor mice treated with PST001, Dox and PST-Dox in groups 2, 3, and 4. Significance shown is for PST-Dox mice *vs.* respective control group.

days. As shown in Figure 6*C*, *i.p.* administration of PST-Dox showed an ILS of 100 ± 1.8%, while PST001 and Dox yielded only 37.5 ± 2% and 66.6 ± 2.1% respectively. However, in the case of *i.t.* administration, PST-Dox nanoparticles showed a peak ILS of 139 ± 1.8%, followed by 78.9 ± 1.9% (Dox) and 42 ± 2.1 % (PST001).

The Kaplan-Meier survival curves for *i.p.* and *i.t.* modes of different drugs in EAC solid tumor bearing mice are shown in Figure 6*D*. Among the three drugs tested, it is obvious that PST-Dox nanoparticles were the most efficient yielding a significant solid tumor regression and increment in life span on *i.t.* administration
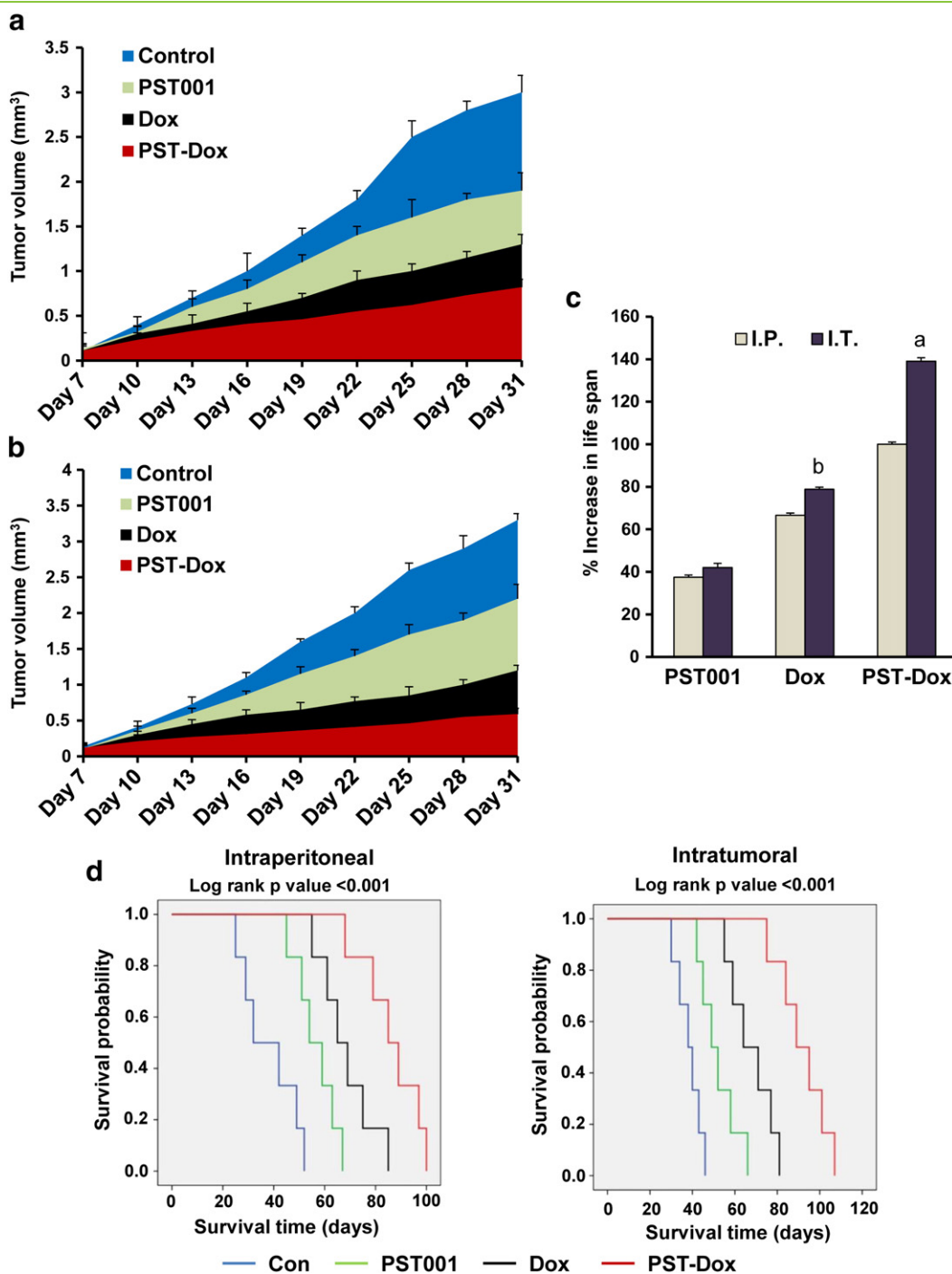
Figure 6. Efficacy of various compounds against EAC solid tumors in mice. EAC cells were injected subcutaneously in the hind limbs to develop solid tumors in mice. Compounds were injected either **(a)** intraperitoneally (*i.p.*) or **(b)** intratumorally (*i.t.*) for the entire duration of the experiment. Solid-tumor measurements were taken every three days starting from day 7 until day 31 as shown. Statistical significance was achieved for PST-Dox *vs.* control group from day 13 on intratumoral administration ($P < .01$) and from day 16 on intraperitoneal administration ($P < .01$) **(c)** Increment in life span was calculated in EAC-induced solid-tumor bearing mice with respect to different routes of drug administration. Results are expressed as the mean $\pm$ SD of the group. Statistically significant differences at a, $P < .001$ and b, $P < 0.01$ compared to the other route. **(d)** Kaplan-Meier survival curves of EAC-induced solid-tumor bearing mice administered with *i.p.* or *i.t.* administration of PST001 or Dox or PST-Dox nanoparticles. Significance shown is for PST-Dox mice *vs.* respective control group.

compared to *i.p.* administration. As observed earlier, even in the solid tumors, Dox treatment showed the second best overall effect, followed by PST001. But, it is interesting to note that there were no differences in the trends of tumor reduction between the parent compounds, PST001 and Dox (Figure 6A *vs. B*) on either mode of drug administration.

Ascites tumor is the direct nutritional source for tumor cells, and an increased volume indicates the need to meet the nutritional

requirements of growing tumor cells [39]. Evaluation of the anticancer potential in mice models showed significant reduction in the ascites tumor volume as evidenced in various experimental groups. Treatment with PST-Dox nanoparticles significantly reduced the tumor volume, viable tumor cell counts, and increased lifespan in both the ascites and solid tumor models. The idea of delivering drugs intratumorally has not been evaluated much in the area of carrier based therapeutics. However, it results in the increased drug concentration at the specific target sites while minimizing the local toxicity [40,41]. Hence, an improvement in the therapeutic index is expected. In our context, administration of nanoparticles *via* intratumoral route delivered higher response than the intraperitoneal route, but no such variation was observed in the case of PST001 and Dox. This could be owing to the phenomenon of tumor leakage exhibited by the bulk molecules. Although larger macromolecules displayed the highest accumulation in tumors, they penetrated only a relatively short distance into the tumor and were mostly concentrated near the vascular surface [42]. It has been proposed that nanoparticles demonstrated increased cytotoxicity by 'enhanced permeation and retention' (EPR) relative to the parent polymer through which they tend to be accumulated at the tumor sites, delivering better responses with less deleterious effects. Importantly, tumor is accompanied with acidosis and tumor microenvironment will follow a drastic drop in pH compared with the surrounding niche. Hence, in the case of hydrophilic polymers like PST001, EPR will enable the accumulation of PST-Dox nanoparticles and release of Dox preferentially at the tumor target sites. This aspect was noticed with the release kinetics performed on human cancer cell lines such as HCT116, MCF-7 and K562 for the measurement of intracellular Dox. Also, both the confocal measurement and flurimetric estimation clearly demonstrate the increased accumulation of Dox from the PST-Dox nanoparticles compared to the naked Dox-Hcl.

Prolongation of lifespan in animals with an ILS exceeding 25% indicated antitumor effectiveness of a drug as per NCI criteria [25]. The tumor reduction exhibited by PST-Dox nanoparticle was higher than the clinically used counterpart Dox, and the overall survival was also the longest than many known chemotherapeutics. This superior effect combined with less toxicity could be attributed to the already reported immunomodulatory effects of PST001 [22] in the nanoparticle formulation. Most chemotherapeutic agents have serious side-effects which limit their widespread clinical applications, warranting the need for anticancer agents that are non-toxic to normal cells. We recently reported the tumor specificity and reduction in the Dox organ-related toxicity in galactoxyloglucan-Dox conjugated nanoparticles [26]. In the current study also, there were no observable side-effects upon administration of the parent polysaccharide as well as its nanoparticle derivative, which justifies their unique drug utility. PST-Dox nanoparticles maintained the safety profile of the immunostimulatory polysaccharide, PST001 while eliciting anticancer potential of both Dox and PST001. Thus, our data suggests that PST-Dox nanoparticle is a better alternative to the clinically available Dox in all the aspects, with respect to limiting both solid and ascites tumors.

Conclusions

This study demonstrates the promising anticancer potential of a nanoparticle aggregate of doxorubicin, PST-Dox. Galactoxyloglucan nanoparticles carrying the Dox moiety significantly decreased cell viability of murine ascites by the induction of apoptosis in the monolayer culture. The cellular uptake of the PST-Dox also showed encouraging results in the colon and breast cancer cells compared to the uptake from the free Dox. In the ascites tumors, PST-Dox increased survival by reducing the tumor burden, especially in early, later and prophylactic phases of ascites tumors. In particular, they were very effective intratumorally against solid tumors. This indeed will extend the drug utility of PST-Dox for more intensive loco regional applications without causing any non-specific toxicity, especially in the case of easily accessible solid malignancies. Agents like PST-Dox deliver multiple effects at the local tumor sites without any side-effects, and offer better flexibility for cancer treatment optimization. Although higher animal models and more mechanistic studies are warranted, PST-Dox has the potential to substantially improve the therapeutic outcome in several malignancies as evidenced. Hence, PST-Dox nanoparticles should be considered as an alternative to Dox in the mainstream chemotherapy.

Supplementary data to this article can be found online at http://dx.doi.org/10.1016/j.tranon.2014.07.003.

References

[1] Masui K, Gini B, Wykosky J, Zanca C, Mischel PS, Furnari FB, and Cavenee WK (2013). A tale of two approaches: complementary mechanisms of cytotoxic and targeted therapy resistance may inform next-generation cancer treatments. *Carcinogenesis* **34**, 725–738.

[2] Rose AJ, Sreelekha TT, and George SK (2013). Nanostrategies in the war against multidrug resistance in leukemia. *Onco Drugs* **1**, 3e–9e.

[3] Von DDH, Layard MW, Basa P, Davis HL, Von ALH, Rozencweig M, and Muggia FM (1979). Risk factors for doxorubicin-lnduced congestive heart failure. *Ann Intern Med* **91**, 710–717.

[4] Chen J, Ling R, Yao Q, Li Y, Chen T, Wang Z, and Li K (2005). Effect of small-sized liposomal Adriamycin administered by various routes on a metastatic breast cancer model. *Endocr Relat Cancer* **12**, 93–100.

[5] Safra T, Muggia F, Jeffers S, Groshen S, Lyass O, Henderson R, Berry G, and Gabizon A (2000). Pegylated liposomal doxorubicin (doxil): reduced clinical cardiotoxicity in patients reaching or exceeding cumulative doses of 500 mg/m2. *Ann. Oncol* **11**, 1029–1033.

[6] Hyuk Sang KHLY, Jong OE, and Tae GP (2000). In vitro and in vivo anti-tumor activities of nanoparticles based on doxorubicin-PLGA conjugates. *J Control Release* **68**, 419–431.

[7] Addeo RFV, Guarrasi R, Montella L, Vincenzi B, Capasso E, Cennamo G, Rotundo MS, Tagliaferri P, Caraglia M, and Del PS, et al (2008). Liposomal pegylated doxorubicin plus vinorelbine combination as first-line chemotherapy for metastatic breast cancer in elderly women > or = 65 years of age. *Cancer Chemother Pharmacol* **65**, 285–292.

[8] Couvreur P and Vauthier C (2006). Nanotechnology: intelligent design to treat complex disease. *Pharm Res* **23**, 1417–1450.

[9] Ruenraroengsak P, Cook JM, and Florence AT (2010). Nanosystem drug targeting: facing up to complex realities. *J Control Release* **141**, 265–276.

[10] Wang AZ, Gu F, Zhang L, Chan JM, Radovic AM, Shaikh MR, and Farokhzad OC (2008). Biofunctionalized targeted nanoparticles for therapeutic applications. *Expert Opin Biol Ther* **8**, 1063–1070.

[11] Elsabahy M and Wooley KL (2012). Design of polymeric nanoparticles for biomedical delivery applications. *Chem Soc Rev* **41**, 2545–2561.

[12] Kumari A, Yadav SK, and Yadav SC (2010). Biodegradable polymeric nanoparticles based drug delivery systems. *Colloids Surf B Biointerfaces* **75**, 1–18.

[13] Greco F and Vicent MJ (2009). Combination therapy: opportunities and challenges for polymer–drug conjugates as anticancer nanomedicines. *Adv Drug Deliv Rev* **61**, 1203–1213.

[14] Lammers T, Kiessling F, Hennink WE, and Storm G (2012). Drug targeting to tumors: principles, pitfalls and (pre-) clinical progress. *J Control Release* **161**, 175–187.

[15] Lammers T, Subr V, Ulbrich K, Peschke P, Huber PE, Hennink WE, and Storm G (2009). Simultaneous delivery of doxorubicin and gemcitabine to tumors in vivo using prototypic polymeric drug carriers. *Biomaterials* **30**, 3466–3475.

[16] Zhang L, Radovic AFM, Alexis F, Gu FX, Basto PA, Bagalkot V, Jon S, Langer RS, and Farokhzad OC (2007). Co-Delivery *of Hydrophobic and Hydrophilic Drugs from Nanoparticle–Aptamer Bioconjugates*. *ChemMedChem* **2**, 1268–1271.

[17] Aryal S, Hu CMJ, and Zhang L (2011). Polymeric nanoparticles with precise ratiometric control over drug loading for combination therapy. *Mol Pharm* **8**, 1401–1407.

[18] Greish K (2007). Enhanced permeability and retention of macromolecular drugs in solid tumors: a royal gate for targeted anticancer nanomedicines. *J Drug Target* **15**, 457–464.

[19] Yokoyama M, Miyauchi M, Yamada N, Okano T, Sakurai Y, Kataoka K, and Inoue S (1990). Characterization and anticancer activity of the micelle-forming polymeric anticancer drug adriamycin-conjugated poly (ethylene glycol)-poly (aspartic acid) block copolymer. *Cancer Res* **50**, 1693–1700.

[20] Jong WHD and Borm PJ (2008). Drug delivery and nanoparticles: applications and hazards. *Int J Nanomedicine* **3**, 133–149.

[21] Sreelekha TT, Vijayakumar T, Ankanthil R, Vijayan KK, and Nair MK (1993). Immunomodulatory effects of a polysaccharide from Tamarindus indica. *Anticancer Drugs* **4**, 209–212.

[22] Aravind SR, Manu MJ, Varghese S, Balaram P, and Sreelekha TT (2012). Antitumor and immunopotentiating activity of polysaccharide PST001 isolated from the seed kernel of Tamarindus indica: an in vivo study in mice. *Sci World J* **2012**, 1–14.

[23] Aravind SR, Manu MJ, Varghese S, Balaram P, and Sreelekha TT (2012). Polysaccharide PST001 isolated from the seed kernel of Tamarindus indica induces apoptosis in murine cancer cells. *Int J Life Sci Pharm Res* , 159–172.

[24] Manu MJ, Aravind SR, Varghese S, Mini S, and Sreelekha TT (2013). PST-Gold nanoparticel as an effective anticancer agent with immunomodulatory properties. *Colloids Surf B Biointerfaces* **104**, 32–39.

[25] Manu MJ, Aravind SR, George SK, Pillai KR, Mini S, and Sreelekha TT (2014). Antitumor activity of galactoxyloglucan-gold nanoparticles against murine ascites and solid carcinoma. *Colloids Surf B Biointerfaces* **116**, 219–227.

[26] Manu MJ, Aravind SR, George SK, Pillai KR, Mini S, and Sreelekha TT (2014). Galactoxyloglucan-modified nanocarriers of doxorubicin for improved tumor-targeted drug delivery with minimal toxicity. *J Biomed Nanotechnol* **10**, 3253–3268.

[27] Dubois M, Gilles K, Hamilton JK, Rebers PA, and Smith F (1956). Colorimetric methods for determination of sugars and related substances. *Anal Chem* **28**, 350–356.

[28] Mosmann T (1983). Rapid colorimetric assay for cellular growth and survival: application to proliferation and cytotoxicity assays. *J Immunol Methods* **65**, 55–63.

[29] McGahon AJ, Martin SJ, Bissonnette RP, Mahboubi A, Shi Y, Mogil RJ, Nishioka WK, and Green DR (1995). The end of the (cell) line: methods for the study of apoptosis in vitro. *Methods Cell Biol* **46**, 153–185.

[30] Wong HL, Ranth AM, Bendayan R, Manias LJ, Ramaswamy M, Liu Z, Erhan SZ, and Wu XY (2006). A New polymer -lipid hybrid nanoparticel system increases cytotoxicity of doxorubicin against multidrug-resistant human breast cancer cells. *Pharm Res* **23**, 1574–1585.

[31] Robert Jan GAKV, Albert VH, Shuraila Z, Stefan RV, Storm G, Vereij M, and Blitterswijk W J (2005). Conformulated N-Octanoyl-glucosylceramide Improves Cellular Delivery and Cytotoxicity of Liposomal Doxorubicin. *Pharmacol. Exp. Ther* **315**, 704–710.

[32] Manu MJ, Aravind SR, George SK, Varghese S, and Sreelekha TT (2013). A galactomannan polysaccharide from Punica granatum impartsin vitro and in vivo anticancer activity. *Carbohydr Polym* **98**, 1466–1475.

[33] Atia MA and Weiss WD (1996). Immunology of spondaneous mammary carcinomas in mice. Acquired tumor resisitance and enhancement in strain A mice infected with mammary tumor virus. *Cancer Res* **26**, 1887–1900.

[34] Ooi VE and Liu F (2000). Immunomodulation and anti-cancer activity of polysaccharide-protein complexes. *Curr Med Chem* **7**, 715–729.

[35] Niu G, Zhu L, Ho DN, Zhang F, Gao H, Quan Q, Hida N, Ozawa T, Liu G, and Chen X (2013). Longitudinal bioluminescence imaging of the dynamics of Doxorubicin induced apoptosis. *Theranostics* **3**, 190–200.

[36] Yang F, Tang Q, Zhong X, Bai Y, Chen T, Zhang Y, Li Y, and Zheng W (2012). Surface decoration by Spirulina polysaccharide enhances the cellular uptake and anticancer efficacy of selenium nanoparticles. *Int J Nanomedicine* **7**, 835–844.

[37] Naguib YW and Cui Z (2014). Nanomedicine: the promise and challenges in cancer chemotherapy. *Adv Exp Med Biol* **811**, 207–233.

[38] Lin YYJ, Shigdar S, Fang DZ, Du JR, Ming QW, Andrew D, Liu K, and Duan W (2012). Enhanced antitumor efficacy and reduced systemic toxicity of sulfatide-containing nanoliposomal doxorubicin in a xenograft model of colorectal cancer. *PLoS One* **7**, 1–10.

[39] Prasad SB and Giri A (1994). Antitumor effects of cisplatin against murine ascites Dalton's lymphoma. *Indian J Exp Biol* **32**, 155–162.

[40] Akporiaye ET and Hersh E (1999). Clinical aspects of intratumoral gene therapy. *Curr Opin Mol Ther* **1**, 443–453.

[41] Neyns B and Noppen M (2003). Intratumoral gene therapy for non-small cell lung cancer: current status and future directions. *Monaldi Arch Chest Dis* **59**, 287–295.

[42] Matthew R, Dreher WL, Michelich CR, Dewhirst MW, Yuan F, and Chilkoti A (2006). Tumor vascular permeability, accumulation, and penetration of macromolecular drug carriers. *J Natl Cancer Inst* **98**, 335–344.